Laboratory Investigation (2013) 93, 528–542

A three-dimensional microenvironment alters protein expression and chemosensitivity of epithelial ovarian cancer cells *in vitro*

Janet Myungjin Lee[1], Paulette Mhawech-Fauceglia[2], Nathan Lee[1], Lucineh Cristina Parsanian[1], Yvonne Gail Lin[3], Simon Andrew Gayther[1] and Kate Lawrenson[1]

For many cancers, there is a real need for more effective therapies. Although many drugs show promising results *in vitro*, most fail to translate into an *in vivo* model system, and only ~5% show anti-tumor activity in clinical trials. It remains a significant challenge to accurately replicate *in vitro* the complex *in vivo* microenvironment in which cancers thrive, but this will be key to increasing the success of translating novel therapies into clinical practice. Three-dimensional (3D) cell culture models may better mimic primary tumors *in vivo* than traditional two-dimensional (2D) cultures. Therefore, we established and characterized 3D *in vitro* models of 31 epithelial ovarian cancer (EOC) cell lines, compared their biological and molecular features with 2D cultures and primary tumors, and tested their efficacy as models for evaluating chemoresponse. When cultured in 3D using polyhydroxoethylamethacrylate-coated plastics, EOC lines formed multicellular aggregates that could be classified as 'large dense', 'large loose', and 'small', based on size, light permeability, and proportion of cells incorporated into the complex structures. Features of histological differentiation characteristic of primary tumors that were not present in 2D cultures were restored in 3D. For many cell lines, the transition from a 2D to 3D microenvironment induced changes in the expression of several biomarkers relevant to disease. Generally, EOC cell lines proliferated more slowly and were more chemoresistant in 3D compared with 2D culture. In summary, 3D models of EOCs better reflect the histological, biological, and molecular features of primary tumors than the same cells cultured using traditional 2D techniques; 3D *in vitro* models also exhibit different sensitivities to chemotherapeutic agents compared with 2D models, which may have a significant impact on the success of drug testing pipelines for EOC. These findings could also impact *in vitro* modeling approaches and drug development strategies for other solid tumor types.
Laboratory Investigation (2013) **93,** 528–542; doi:10.1038/labinvest.2013.41; published online 4 March 2013

KEYWORDS: epithelial ovarian cancer; three-dimensional modeling; cell adhesion; chemoresponse; microenvironment; chemoresistance

The success rate of anti-cancer therapies translating from *in vitro* culture systems into the clinic is about 5%.[1] The vast majority of drugs that show promising results *in vitro* fail to replicate in an *in vivo* model system and even fewer make it into clinical trials. Nonetheless testing drugs in cell culture models is a vital part of any drug development process. It is likely that a major contributing factor to the low rates of *in vivo* translation of new therapeutic agents is the widespread use of two-dimensional (2D) monolayer culture systems used for *in vitro* drug discovery and development. 2D cultures fail to recapitulate the gradients of drugs, nutrients, gases, and waste products that characterize tumors *in vivo*; all are important factors influencing response to therapy.[2,3] Moreover, many of the signaling pathways involved in chemoresponsiveness are differentially activated in monolayer cultures, and as a result, 2D cultures are often more sensitive to drug therapies yielding many false-positive results in 2D drug screens.[4,5] Conversely, it is highly likely that many effective therapeutic agents may have been missed owing to false-negative reporting in 2D drug tests.

An alternative approach to drug testing is to use three-dimensional (3D) cell culture models. 3D culturing of cells

[1]Department of Preventive Medicine, University of Southern California/Keck School of Medicine, Los Angeles, CA, USA; [2]Departments of Medicine and Pathology, University of Southern California/Keck School of Medicine, Los Angeles, CA, USA and [3]Department of Obstetrics and Gynecology, University of Southern California/Keck School of Medicine, Los Angeles, CA, USA
Correspondence: Dr K Lawrenson, PhD, Department of Preventive Medicine, University of Southern California/Keck School of Medicine, NRT2517H, 1450 Biggy Street, Norris Research Tower, Los Angeles, CA 90033, USA.
E-mail: Kate.Lawrenson@med.usc.edu

Received 15 September 2012; revised 21 December 2012; accepted 24 January 2013

can be achieved by culturing primary tissues or established cell lines within extracellular matrix gels, synthetic scaffolds, rotary cell culture systems, or on low/non-adherent culture plastics;[6–11] these 3D cell culture techniques all aim to restore the 3D architecture that characterizes normal tissues and solid tumors alike. Studies have shown that gene expression profiles of 3D-cultured cells are dramatically different to monolayer cultures and more closely resemble the profiles of the tissues of origin than their 2D counterparts.[11–14] 3D multicellular aggregate (MCA) structures also contain many features absent in 2D cultures that are present in primary tissues. For example, in MCAs of tumor cells hypoxic and necrotic areas can develop, regions that are commonly found in primary tumors and known to be associated with chemoresistance.[15]

Despite the fact that 3D cell culture models better recapitulate primary tumors than monolayer systems, 3D approaches have not yet been universally integrated into the drug development arena because of traditionally higher costs, greater technical challenges, and perceived lower rates of reproducibility than classical monolayer approaches. In the past decade, considerable advances have been made to establish cheaper and reliable methodologies for high-throughput phenotypic evaluation of cultured cells in 3D for drug development.[16,17] The continued hesitation to use 3D models for drug development more widely may largely be due to the limited data available detailing the changes in cellular phenotypes following the transition from a 2D to a 3D microenvironment. Many cell lines have not yet been well characterized as 3D models, and so systematic phenotypic evaluation of large numbers of cell lines is required to facilitate the use of those cell lines in 3D drug screening studies.

Epithelial ovarian cancer (EOC) is the leading cause of death from gynecological malignancy in Western societies. With the exception of anti-vascular agents and PARP inhibitors,[18,19] there has been limited progress in the development of novel approaches to treating EOC over the past 40 years; consequently, survival rates have only shown minimal improvement. Although most EOCs initially respond well to platinum-based chemotherapy, median progression free survival is only 18 months[20] as chemoresistant recurrent disease commonly evolves and is usually fatal.

There is an urgent clinical need for more effective therapeutic targets that can be integrated into the treatment of advanced EOCs, and for the discovery of new drugs that show higher rates of translatability. Here, we report on the characterization of thirty-one EOC cell lines grown as 3D MCAs under static non-adherent conditions. We evaluated changes in protein expression of cell adhesion molecules and ovarian cancer biomarkers and found that EOC cells cultured in 3D differentially express adherens junction proteins and are frequently more chemoresistant than the same cells cultured as 2D monolayers. These data suggest that *in vitro* 3D models of EOC represent a biologically relevant platform for studying ovarian cancer cell biology, tumorigenesis, and for accelerating the development of novel therapeutic targets.

MATERIALS AND METHODS

Cell Culture

EOC cell lines were maintained in the appropriate growth media (Supplementary Table S1). Cell lines were obtained from the ATCC or were a kind gift from Dr G Mills at MD Anderson. All cell lines were confirmed to be free of *Mycoplasma* infection. To create 3D spheroids, tissue culture dishes were coated twice with 1.5% polyhydroxoethylamethacrylate (polyHEMA; Sigma) dissolved in 95% ethanol (VWR). Coated dishes were allowed to dry completely before use. Cells were trypsinized, resuspended in the appropriate growth medium, and inoculated into a polyHEMA-coated plate that had first been washed with $1 \times$ PBS for 5 min. Cell cultures were re-fed every 3–4 days. Phase images were acquired using a Nikon Eclipse TS100 microscope and NIS Elements D 3.2 software.

In vivo Xenograft Assays

All *in vivo* work was performed under the approval and guidance of the University of Southern California Institutional Animal Care and Use Committee. 3×10^6 ovarian cancer cells were resuspended in sterile phosphate-buffered saline (PBS) and injected intra-peritoneally or subcutaneously into 6–7 week-old nu/nu mice (Simonsen Laboratories). At humane endpoints, mice were killed by CO_2 inhalation followed by cervical dislocation. Tissues were harvested and fixed in neutral-buffered formalin. Hematoxylin and eosin staining was performed at the USC Surgical Pathology Laboratory.

Immunohistochemistry (IHC)

For IHC, 3D cultures were taken at day 14 and spun at 200 *g* to sediment the spheroids. 2D cultures were spun for 5 min at 450 *g* to create a cell pellet, which was then loosened by flicking the tube. Cell culture samples or murine tissue specimens were washed in $1 \times$ PBS and fixed for 30 min in neutral-buffered formalin (VWR). Samples were rewashed twice in $1 \times$ PBS and transferred to 70% ethanol. Fixed spheroids and cell suspensions were resuspended in 1% agarose dissolved in PBS to create uniformly sized specimens for embedding. Specimens were processed into paraffin and hematoxylin-stained sections prepared at the USC Translational Pathology Core Facility, using standard techniques. 2D/3D tissue microarrays (TMA) were also created at the USC Translational Pathology Core Facility. One 2 mm core was taken per cell line for each culture condition and embedded into the recipient block. TMA sections were stained by IHC, using the BOND III automated stainer (Leica Microsystems), by the USC Immunohistochemistry Laboratory within the USC Department of Pathology. The following antibodies were used: Cleaved caspase 3 (cat no: 9664, Cell Signaling, clone D175 &

5AIE); WT-1 (cat no: WT1-562-L-CE, Leica Microsystems, clone WT49); Pan Keratin (cat no: AE1/AE3-L-CE, Leica Microsystems, clone AE1/AE3); Vimentin (cat no: VIM-572-L-CE, Leica M., clone SRL 33); ER (cat no: NCL-ER-6F11, Novacastra, clone 6F11); PR (cat no: PGR-312-L-F, Novocastra, clone PGR-312); Ki-67 (cat no: IR626, Dako Corporation, clone MIB-1); Beta-catenin (cat no: B-CAT-U, Leica M., clone 17C2); E-cadherin (cat no: E-CAD-L-CE, Leica M., clone 36B5); CA125 (cat no: CA125-CE, Leica M., clone OV185.1); PAX8 (cat no: ACI 438, Biocare, clone BC12); and P53 (cat no: P53-DO1, Leica M., D07). Stained slides were scanned with Aperio ScanScope CS and ImageScope software with a $\times 20$ lens with $\times 2$ multiplier lens at the Cell and Tissue Imaging Core at USC.

Immunoblotting

Monolayer cultured cells at 80% confluency or 14-day-old 3D cell spheroids were washed twice with cold PBS and lysed with lysis buffer (20 mM TrisCl, pH 7.5; 150 mM NaCl; 1% Triton-X 100; 1.2 mg/ml aprotinin; 10 mg/ml leupeptin; 1 mM PMSF; all Sigma-Aldrich) by rotation at 4 °C for 20 min. The cell debris was cleared by centrifugation at 14,000 rpm for 10 min. Post quantification, by a Bradford Assay (Pierce), the lysates were boiled in Laemmli SDS sample buffer (50 mM Tris, pH 6.8;, 10% glycerol; 2% SDS; 0.1% bromophenol blue; 5% β-mercaptoethanol; all Sigma-Aldrich) for 5 min. The lysates were resolved by SDS-PAGE and transferred to a PVDF membrane (Pall Life Science). The membranes were blocked with 50% Odyssey Blocking Buffer (Li-Cor Biosciences) in PBS for 1 h at room temperature. The membranes were then incubated for a minimum of 1 h in the following antibodies, all diluted 1:1000 in Odyssey blocking buffer containing 0.2% Tween: anti-P-Cadherin monoclonal antibody (cat no: 32–4000, Invitrogen), anti-N-cadherin monoclonal antibody (cat no: 33-3900, Invitrogen), anti-E-Cadherin monoclonal antibody (cat no: 04-1103, Millipore), anti-Integrin beta 1 monoclonal antibody (cat no: 04-1109, Millipore), anti-b-catenin polyclonal antibody (cat no: sc-7199, Santa Cruz Biotechnology), anti-pan-Cytokeratin monoclonal antibody (cat no: sc-8018, Santa Cruz Biotechnology), anti-vimentin monoclonal antibody (cat no: CBL202, Millipore), or anti-actin polyclonal antibody (cat no: A 5060, Sigma-Aldrich). For detection of the proteins, membranes were probed with the appropriate Odyssey IRDye-coupled secondary antibodies that emit at either 680 nm or 800 nm and proteins detected using the Odyssey IR Detection System (Li-Cor Biosciences).

3D Cell Proliferation Assays

In all, 1×10^3 cells were seeded, in six replicates, into 96-well plates for 2D monolayers, and also into 1.5% polyHEMA-coated 96-well plates for 3D spheroids. Prestoblue (Invitrogen) was added to the cells on the day of plating, and the fluorescence from the reduced resazurin was read 3 h post seeding and every 24 h thereafter.

Chemotherapeutic Response Assays

In all, 5×10^3 cells were seeded in 96-well plates, in quadruplet. For 3D cultures, cells were seeded into 96-well plates that had been twice pre-coated with 1.5% polyHEMA. Cells were allowed to adhere to the dish or form spheroids for 24 h, at which point 0.1 mg/ml cisplatin or 100 nM paclitaxel was administered. After 48 h, Prestoblue (Invitrogen) was added to the cells, incubated at 37 °C for 3 h, and the fluorescence measured using a Mikrowin platereader.

RESULTS

3D Models of Ovarian Cancer Cell Lines Exhibit Distinct Spheroid Morphologies

We established thirty-one EOC cell lines as *in vitro* 3D spheroid models by culturing cells on polyHEMA-coated tissue culture plastics for 14 days (Table 1).[9,11] Cell lines were epithelial and had been established either from primary tumors, ascites, or metastases and represented the main histological subtypes of EOC, namely serous, endometrioid, clear cell, and mucinous ovarian cancer. All cell lines, with the exception of OVCA429 and OVCA433, formed MCA structures under static culture conditions. EOC cell lines propagated in a 3D microenvironment exhibited strikingly distinct MCA morphologies. Phase-contrast microscopy was used to analyze live cell structures and hematoxylin and eosin staining of paraffin-embedded sections of 3D spheroids was used to characterize the internal architecture of the MCAs. On this basis, EOC cultures were classified into three distinct categories: large dense aggregates (LDAs), large loose aggregates (LLAs), and small aggregates (SAs) (Figure 1 and Table 1).

Nine cell lines (29%) (1847, 1847-AD, ES-2, HEY, HEY.A8, LK2, OAW42, SKOV3, and SKOV3.ip) formed LDAs, which were characteristically large, tightly packed spheroids, 200–800 μm in diameter. Under phase microscopy, LDAs were less light-permeable than the other types of 3D aggregates. Hematoxylin and eosin staining showed that the cores of LDAs could be cellular (eg, HEY.A8) or acellular (eg, OAW42 and 1847). Acellular regions appeared to result from cell death or necrosis, as indicated by nuclear morphologies. Some cell lines produced eosinophilic matrix material (eg, 1847 and HEY.A8). Thirteen cell lines (42%) (COV434, COV644, EFO27, FUOV1, IGROV1, OC316, OV2008, OV2008.C13, OVCAR3, OV-MZ-15, TOV112D, TOV21G, and UWB1.289 + BRCA1) formed LLAs, which were similar in size to LDAs though cells in LLAs appeared to be more loosely adhered to neighboring cells than in LDAs and as a result LLAs were more light-permeable. Finally, eight cell lines (26%) formed SAs (A2780, A2780.CP, CaOV3, JAMA2, OVCAR5, OVCAR10, PXN94, and UWB1.289), which were small multicellular structures of loosely attached cells, approximately 50–200 μm in diameter, but often with many single cells remaining unincorporated into an MCA (eg, JAMA2).

Table 1 Ovarian cancer cell line information and 3D grouping

Cell line	Source	Tumor histology	Tumor stage/ grade *in vivo*	Tumour-igenicity	Marker expression	Known mutation	3D morphology	3D histology	Reference
1847	Ovarian tumor	Not known	Not known	Yes			Large dense	PD, high grade	[21]
1847.AD	From 1847, IVR	Not known	Not known	Not known			Large dense	PD, high grade	[22]
A2780	Ovarian tumor	UD	Not known	Yes	vim +, LMWK +, HMWK + EMA + LCA −	PTEN c.383_391del9	Small	SC, high grade	[21]
A2780.CP	From A2780, IVR	UD	Not known	Yes	vim +, LMWK +, HMWK + EMA + LCA −		Small	nd	[23]
CaOV3	POT	Not known	Not known	Yes	CA125 +, Ca-1 +, CEA +, Ba-2 +	FAM123B c.1_2415del2415; STK11 c.1_1302del1302; TP53 c. 406C > T; PTEN (aa p.W274G)	Small	MC[b], high grade	[24]
COV644	POT	MC	Not known	Not known			Large loose	PD, high grade	[25]
EFO27	OM	MC	intermediate	Yes (nude)	LHRH +	MSH2 mut:c.387_388delTC; PTEN c.800delA; TP53 c.817C > T	Large loose	PD, high grade	[26]
ES-2	POT	CCC	PD	Yes	vim +, LMWK +, HMWK + EMA + LCA −	BRAF c.1799T > A; TP53 (aa p.S241F)	Large loose	nd	[27]
FUOV1	XEN	SC	Stage IIIc, PD	Not known		TP53 (aa p.H179D)	Large loose	SC, high grade	
HEY	XEN	SC	MD	Yes	Ba-2	BRAF c.1391G > A	Large dense	PD, high grade	[24]
HEY.A8	XEN	Not known	Not known	Yes			Large dense	PD, high grade	[28]
IGROV1	POT	EC with CCC/UD	Stage III	Yes	EGFR +	MLH1 c.1513delA; MSH6 c.3261delC; TP53 c.377A > G; PIK3CA c.3207A > G; PTEN c.955-958delACTT	Large loose	SC, high grade	[29]
JAMA-2	XEN	SC	PD	Yes	HMFG1 −, HMFG2 −, AUA1 −, F36/22 −, PLAP −		Small	nd	[30]
LK2	AF	Not known	Not known	Not known		APC C.2055G > A; CDKN2A C.250G > T; TP53 C.814G > A; EGFR c.2573T > G; NFE2L2 c.235G > A	Large dense	[a]	[31]
OAW42	AF	PC	Not known	Not known	CA125 −, CEA −	PIK3CA c.3140A > T	Large dense	SC, low grade	[32]
OC316	PM	LD	Stage IV	Yes			Large loose	SC, high grade	[33]
OV2008	XEN	EC*	Not known	Yes	vim +, LMWK +, HMWK + EMA + LCA −	CTNNA1 c.103C > T	Large loose	PD/SQ, high grade	[34]
OV2008.C13	From OV2008, IVR	EC*	Not known	No	vim +, LMWK +, HMWK + EMA + LCA −	Mutant p53	Large loose	PD/SQ, high grade	[35]
OVCA429	POT	Not known	Not known	Yes	CA125 +	CDKN2A c.1_471del471; CDKN2A c.1_150del150; PIK3CA c.1633G > A	Not viable	NA	[36]
OVCA433	POT	Not known	Not known	No	CA125 +	CDKN2A c.1_471del471; CDKN2A c.1_150del150	Not viable	NA	[36]
OVCAR3	AF	Not known	PD		ER +, PR +, AR +		Large loose	PD, high grade	[37]

Table 1 (Continued)

Cell line	Source	Tumor histology	Tumor stage/ grade *in vivo*	Tumour-igenicity	Marker expression	Known mutation	3D morphology	3D histology	Reference
				Yes (athymic), No (CD-1 nude)		RB1 c.2110A>G; PIK3R1 c.1746_1814del69; SMARCA4 c.1208A>G; TP53 c.743G>A			
OVCAR5	AF	Not known	Not known	Yes		CDKN2A c.1_471del471; KRAS c.35G>T; CREBBP c.3211G>A	Small	PD, high grade	[38]
OVCAR10	Ovarian tumor	Not known	Not known	Not known		BRAF c.603G>T; CDKN2 nonsense mutation in exon 2	Small	PD, high grade	[38]
OV-MZ-15	AF	SC	Stage III	No	CA125, CEA		Large loose	PD, high grade	[39]
PXN94	XEN	Not known	Not known	Not known	HMFG2+, CA125+, CEA+	BRAF mutation	Small	SC, high grade	[40]
SKOV3	AF, XEN	Not known	MD	Yes	Blood type B; Rh+	CDKN2A c.1_457del457; CDKN2a(p14) c.317-522del206; MLH1 c.1_2271del2271; PIK3CA c.3140A>G; TP53 c.267celC	Large dense	PD, high grade	[40]
SKOV3.ip	From SKOV3, XEN	Not known	Not known	Yes	HER2/neu+		Large dense	CC, high grade	[41]
TOV112D	POT	EC	Grade 3, Stage IIIC	Yes	HER2/neu+, p53 +	CTNNB1 c.109T>G; p53 mutation: Arg → His mutation at exon 6, codon 175	Large loose	PD, high grade	[42]
TOV21G	POT	CCC	Grade 3, Stage III	Yes	HER2+, p53+ (wild type)	KRAS c.37G>T; PIK3CA c.3139C>T; PTEN c.795delA; ARID1A c.1644_1645insC	Large loose	MC[b], high grade	[42]
UWB1.289	POT	SC	Not known	No	ER−, PR−, Ck7+, Calret+, WT1+, BRCA1-	BRCA1 c.2594delC; TP53 c.625delAG	Small	SC, high grade	[43]
UWB1.289 + BRCA1	From UWB1.289	SC	Not known	No	ER−, PR−, Ck7+, Calret+, WT1+, BRCA1+	BRCA1 c.2594delC; TP53 c.625delAG	Large loose	SC, high grade	[43]

Abbreviations: AF, from ascites; CCC, clear cell carcinoma; EC, endometrioid carcinoma; EC* endometrioid with squamous differentiation; IVR, *in vitro*-induced drug resistance; MC, mucinous carcinoma; MD, moderately differentiated; nd, not done; OM, omental metastasis; PC, papillary cystadenocarcinoma; PD, poorly differentiated; PM, pleural metastasis; POT, primary ovarian tumor; SC, serous carcinoma; SQ, squamous; UD, undifferentiated; WD, well differentiated; XEN, POT grown as xenograft.

A summary of the EOC lines used and their respective 3D morphological grouping is provided. The source, histotype, tumorigenicity, marker expression, and mutational status information obtained from previously published data is cited.

[a]LK2 histology in 3D could not be classified as an ovarian tumor. Mutation data were obtained from the catalog of somatic mutations in cancer (http://cancer.sanger.ac.uk/cancergenome/projects/cosmic/) or from the referenced manuscript; for some cell lines TP53 mutation data were obtained from the cancer cell line encyclopedia (http://www.broadinstitute.org/ccle/) where extensive additional mutation data can be found. Where multiple mutations were found, mutations of known functional significance are shown. Where DNA mutations are not known the change in amino-acid (aa) sequence is given.

[b]Two cell lines displayed histological features suggestive of a mucinous histology that were determined to be artifacts following negative staining for a mucinous marker (cytokeratin 20).

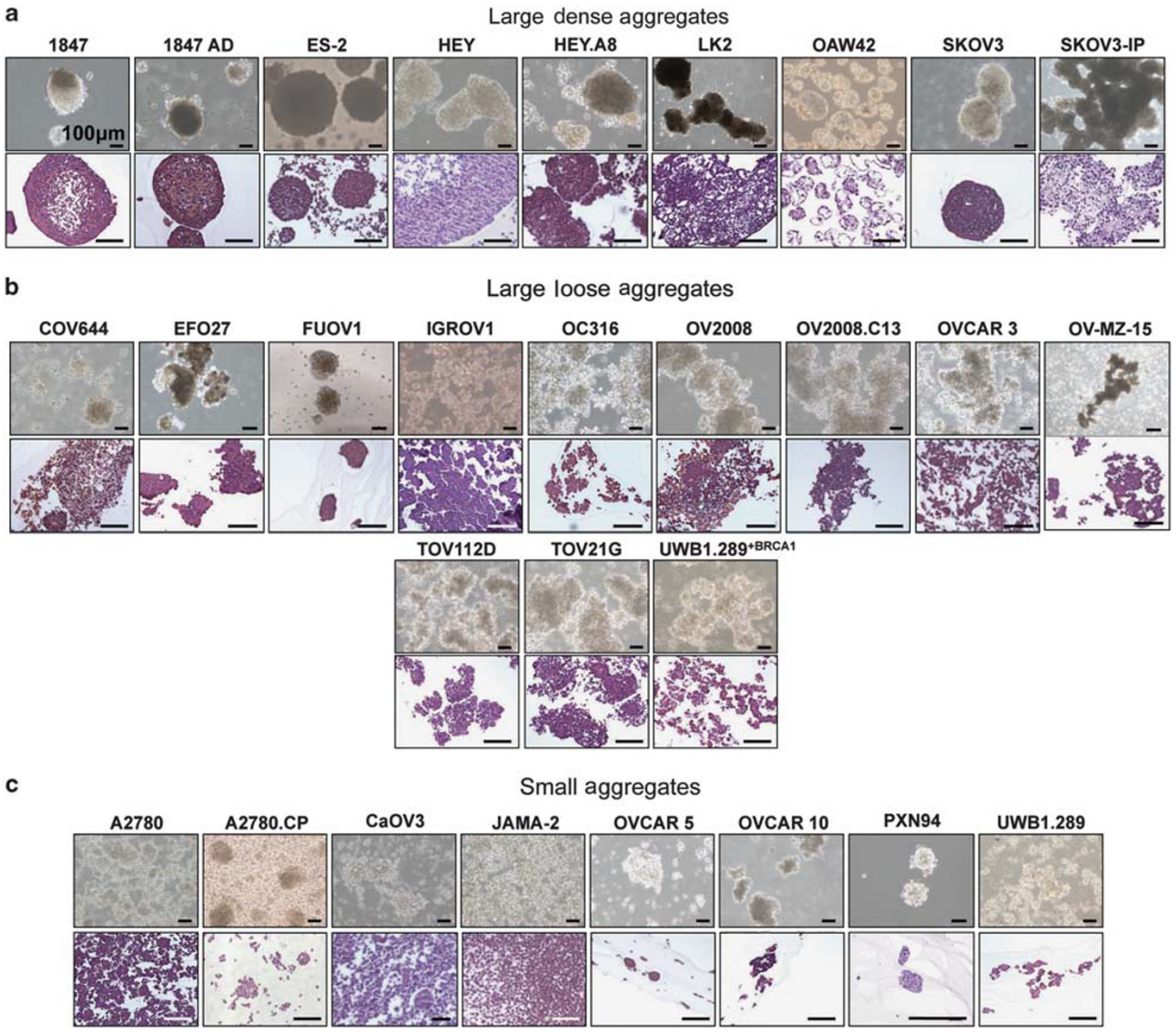

Figure 1 Three-dimensional (3D)-cultured epithelial ovarian cancer cell lines form multicellular aggregates of three different types of morphologies. Spheroid morphologies of 29 epithelial ovarian cancer cell lines cultured in 3D conditions were grouped into three categories: (**a**) Large dense aggregates, (**b**) large loose aggregates and (**c**) small aggregates. Phase contrast and hematoxylin and eosin-stained images of each cell line are shown. Phase and brightfield microscopy.

3D Modeling of EOC Cell Lines Restores Features of Histological Differentiation

2D and 3D cultures of all 29 ovarian cancer cell lines that were viable in 3D were fixed, embedded in paraffin blocks, stained with hematoxylin and eosin, and the histology analyzed. When cultured in 2D monolayers, EOC cell lines do not display any morphological features to indicate histological differentiation that can be detected by phase microscopy. 2D cultured cells were often identifiable as tumor cells, as defined by the morphological criteria in which cell size, nuclear size, nuclear-to-cytoplasmic ratio, prominence of the nucleoli, and the presence of atypical mitotic figures are evaluated; however, complex features of histological differentiation were absent. A number of cell lines displayed obvious histological differentiation in 3D that could not be detected in 2D culture specimens. OAW42 spheroids resembled a well-differentiated (Grade 1) serous ovarian carcinoma and contained psammoma bodies (calcifications), which are found in the primary ovarian serous carcinomas[44] (Figure 2a). Other cell lines (eg, FUOV1, UWB1.289 and UWB1.289 + BRCA1) resembled moderately differentiated (Grade 2) serous carcinomas in 3D (Figure 2b). The majority of the cell lines resembled poorly differentiated (Grade 3) ovarian cancers, which reflects the predominant histology of EOCs at the time of surgery (eg, HEY.A8 shown in Figure 2c; Table 1). For the eight cell lines, the reported histology of the

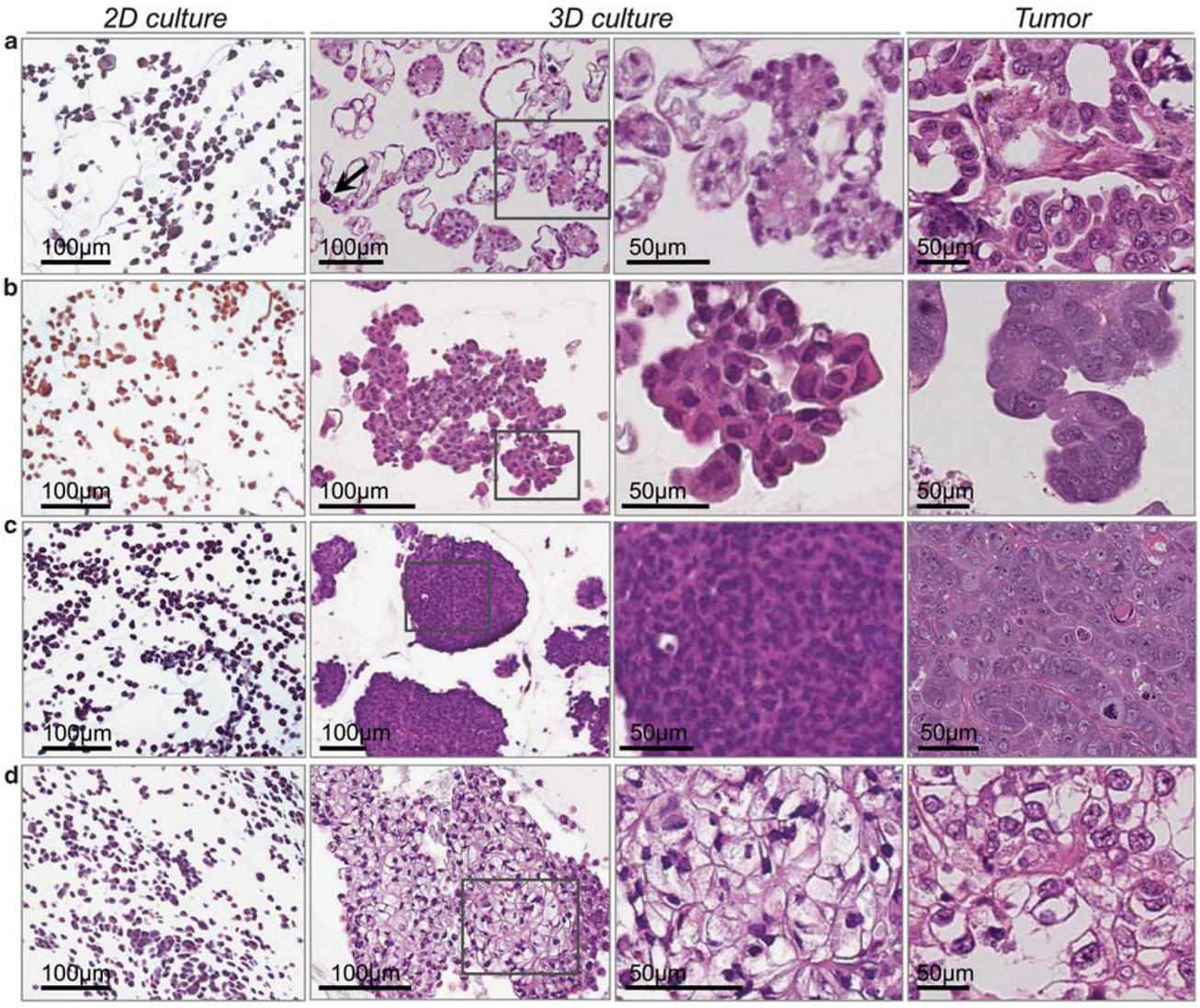

Figure 2 Three-dimensional (3D) culturing of epithelial ovarian cancer (EOC) cell lines better restores features of histological differentiation than traditional two-dimensional (2D) culturing techniques. 2D and 3D cultures were compared with human ovarian carcinoma specimens representative of each tumor histological subtype. Histological analyses revealed that the majority of the EOC cell lines in this study were determined to be of high grade, which was anticipated as the majority of EOC cell lines are derived from high-grade tumors. (**a**) In 3D culture, OAW42 shows classical architecture and histological differentiation of a well-differentiated (Grade 1) serous ovarian tumor. A psammoma body is visible (arrow). The grade of the tumor from which OAW42 was derived is not known; however, in the COSMIC database this cell line is not reported to have a TP53 mutation, suggesting that it is likely this line could have originated from a low-grade serous tumor, as $>95\%$ of high-grade serous tumors harbor TP53 mutations. (**b**) Representative of a moderately well-differentiated serous tumor (Grade 2) is shown by the UWB1.289 + BRCA1 cell line. (**c**) HEY.A8, and example of a cell line that forms MCAs with a poorly differentiated histology (Grade 3). (**d**) SKOV3.ip formed multicellular aggregates (MCAs) that displayed a high-grade clear cell histological differentiation in 3D. Hematoxylin and eosin staining, brightfield microscopy. 3D MCAs were scored using WHO guidelines.

primary tumor was not reflected in the histology of the 3D culture; for example, TOV21G cells are reportedly derived from a clear cell carcinoma, but in 3D cultures resembled a poorly differentiated high-grade carcinoma. SKOV3.ip was the only cell line to form spheroids with characteristics of clear cell carcinoma, characterized by cells with hyperchromatic nuclei, prominent nucleoli, and abundant clear cell cytoplasm (Figure 2d). Interestingly, SKOV3, which is perhaps the most widely used cell line used in cell biology studies of ovarian cancer, is not reported to be derived from a clear cell tumor, although it has been reported that the parental SKOV3 cell line can form tumors of a clear cell histology when xenografted orthotopically into nude mice.[45]

Four EOC cell lines were xenografted, intra-peritoneally or subcutaneously, into immunocompromised mice to compare 3D spheroid cultures to the same cells grown *in vivo*. Two cell

lines (UWB1.289 and UWB1.289 + BRCA1) failed to form tumors. The histologies of the remaining two cell lines (OV2008 and A2780) when grown as 3D spheroids and in xenografts were similar (Figure 3); A2780 cells formed poorly differentiated high-grade serous carcinomas in 3D and in xenograft, whereas OV2008 cells formed squamous cell carcinomas, consistent with a recent report suggesting that this line may be cervical in origin.[46]

Cell Adhesion and Cytoskeletal Protein Expression in 2D and 3D Cultures

When cells are transitioned from a 2D to a 3D microenvironment, cellular shape and the architecture of cell-cell adhesions changes dramatically. We hypothesized that the expression of cell adhesion molecules and cytoskeletal proteins would be altered under 3D culture conditions. Protein lysates were prepared from 2D and 3D cultured EOC cell

a

Cell line	Injection Site	No Cells Injected	Tumor Formation/No Animals	Histology	
				3D Culture	Xenograft
A2780	SC	$3x10^6$	4/4	Serous ovarian ca, high grade	Serous ovarian ca, high grade
OV2008	IP	$3x10^6$	5/5	Squamous cell cervical ca	Squamous cell cervical ca
UWB1.289	SC	$3x10^6$	0/3	Serous ovarian ca, high grade	NA
UWB1.289+BRCA1	SC	$3x10^6$	0/3	Serous ovarian ca, high grade	NA

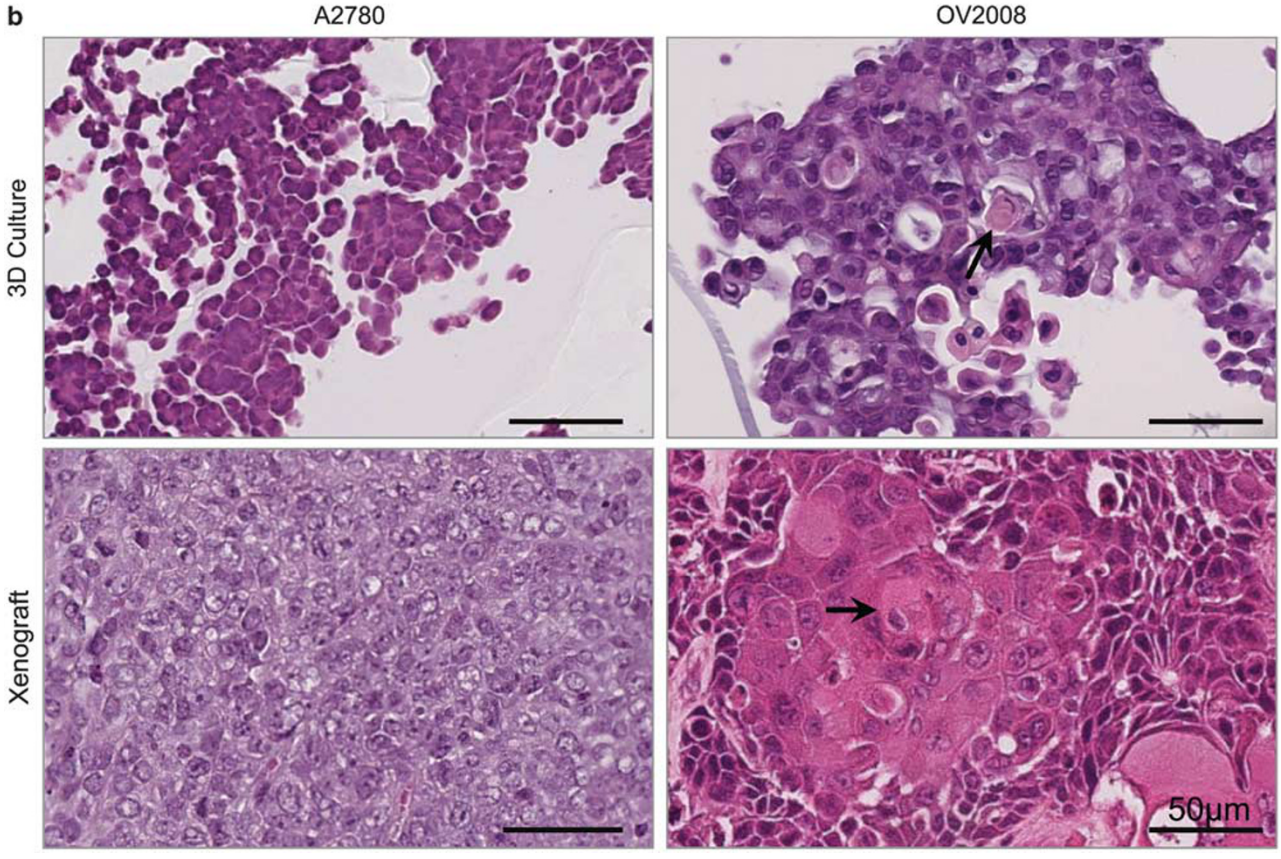

Figure 3 Epithelial ovarian cancer (EOC) cell lines established three-dimensional (3D) cultures and xenografts are histologically similar. (**a**) Four EOC cell lines were xenografted into mice intraperitoneally (IP) or subcutaneously (SC). Two cell lines did not form tumors when 3×10^6 cells were injected, suggesting that these cells are non-tumorigenic in this mouse model or that more cells are required for tumor formation. (**b**) Histology of A2780 and OV2008 cells when grown in 3D and as xenografts. Histological features of 3D and xenografted cells are highly similar. A2780 cells form diffuse sheets of neoplastic cell proliferation in 3D and in xenograft. These cells have high nuclear to cytoplasmic ratio, and multiple mitotic figures, consistent with high-grade serous carcinoma. In 3D and in xenograft OV2008 forms diffuse sheets of neoplastic cells that have a pink, acidophilic cytoplasm and forms keratin pearls (arrow), histologic features consistent with squamous cell carcinoma. There is no glandular structure present. Both xenograft and 3D-cultured cells are highly reminiscent of a cervical carcinoma, in accordance with a recent report which suggested that these cells are cervical in origin.[46]

lines to examine, by western blotting, the expression of several cell adhesion markers (E-cadherin, P-cadherin, and N-cadherin), intermediate filament proteins (pan-cytokeratin and vimentin), and β-catenin, a protein involved in Wnt signaling that is found at the cytoplasmic domain of adherens junctions complexes (Figure 4).

Six of the eight (75%) EOC lines that formed LDAs, 60% of LLAs and 57% of SAs expressed cytokeratin (Figure 4a). Following a transition to a 3D microenvironment, cytokeratin could be both downregulated (LK2, OV2008) and upregulated (eg, OC316, UWB1.289 + BRCA1), although the latter was the most common trend. Vimentin was expressed by 50% of the LDAs, 30% of LLAs, and 43% of SAs (Figure 4b); vimentin expression was more frequently lower in 3D compared with 2D cultures of the same cells. Expression of cytokeratin and vimentin were mutually exclusive in the LLA and SA groups but not in the LDAs. E-cadherin, a cell adhesion molecule expressed in many normal epithelial tissues and in up to 90% of EOCs,[47,48] was expressed by 25% of the LDA-forming lines, 70% of LLAs, and 57% of SAs (Figure 4e). P-cadherin was not expressed by cell lines forming LDAs (Figure 4c) and N-cadherin was expressed by 50% of the lines in this group when cultured in 2D (Figure 4d). About half of cell lines forming LLAs and SAs also expressed either N- or P-cadherin. E-cadherin was always upregulated in 3D compared with 2D cultures, but N- and P-cadherin were most commonly downregulated in 3D. We did not observe a marked trend in the changes of expression of β-catenin in 2D compared with 3D cultures (Figure 4f).

2D- and 3D-Cultured EOC Cells Differentially Express Ovarian Cancer Biomarkers

To analyze the expression of ovarian cancer biomarkers by IHC, we created TMAs of 2D- and 3D-cultured EOC cells. Sections of the TMAs were stained for a panel of ovarian cancer biomarkers (Figure 5), including CA125, a biomarker used clinically to detect ovarian cancer. We preferentially selected additional biomarkers that distinguish between ovarian cancer histological subtypes.[49] MIB1 staining revealed that cells cultured in 3D were less proliferative than cells cultured in 2D, which is similar to previous reports for other cell types.[9,11] We also observed a reduction in p53 expression, which may also reflect the lower proliferation rates of 3D cultured cells. MIB1/p53-positive cells tended to be located in a proliferative zone on the outer surface of the spheroids. Higher expression of active (cleaved) caspase-3 in 3D cultures indicated that 3D MCAs contain a higher proportion of apoptotic cells than 2D-cultured counterparts. Trends in cytokeratin, vimentin, and E-cadherin expression detected by IHC were similar to those detected by western blotting; when expressed, E-cadherin tended to be upregulated and vimentin downregulated in 3D compared with 2D. Generally, there was reduced expression of β-catenin in 3D cultures. When expressed, it was often localized to positive 'zones' in 3D aggregates (Figure 5b). CA125 and PAX8 expression increased and WT1 expression decreased in 3D compared with 2D cultures, although $<30\%$ of cell lines were positive for these markers. No cell lines expressed progesterone receptor and only two cell lines (OV2008, A2780.CP) expressed estrogen receptor at similar levels in 2D and 3D.

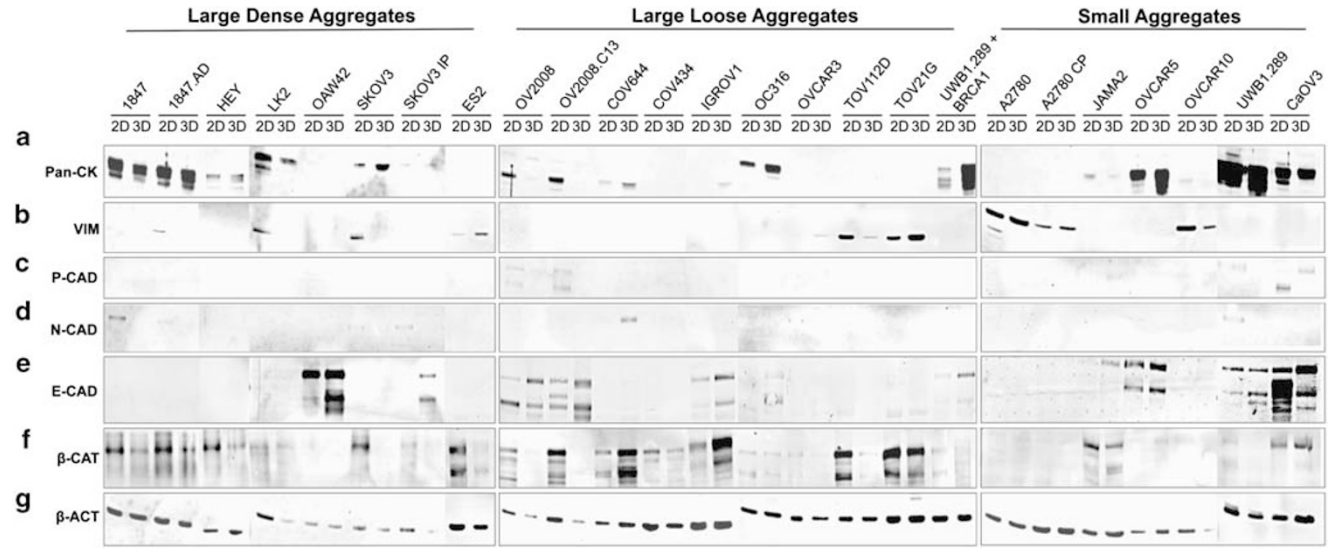

Figure 4 Western blot analysis of the expression of cell adhesion, extracellular matrix, and cytoskeletal proteins in epithelial ovarian cancer (EOC) cultured in two- (2D) and three-dimensional (3D) conditions. Lysates of EOCs propagated in 2D and 3D were immunoblotted for (a) pan-cytokeratin (Pan-CK), (b) vimentin (VIM), (c) P-Cadherin (P-CAD), (d) N-Cadherin (N-CAD), (e) E-Cadherin (E-CAD), (f) β-catenin (β-CAT) and (g) β-actin (β-ACT). In all, 10 mg of protein was loaded for each lane, and β-actin was used as a control. The predominant trends observed (increased E-cadherin expression and reduced vimentin expression) are indicative of a mesenchymal-to-epithelial transition occurring following transition to a 3D microenvironment. In 2D and 3D cultures, we observed differential expression of the full-length 135 kDa and trypsin-resistant 80 kDa E-cadherin proteins as well as other E-cadherin isoforms, suggesting that differential post-translational modification of E-cadherin occurs in 2D and 3D.

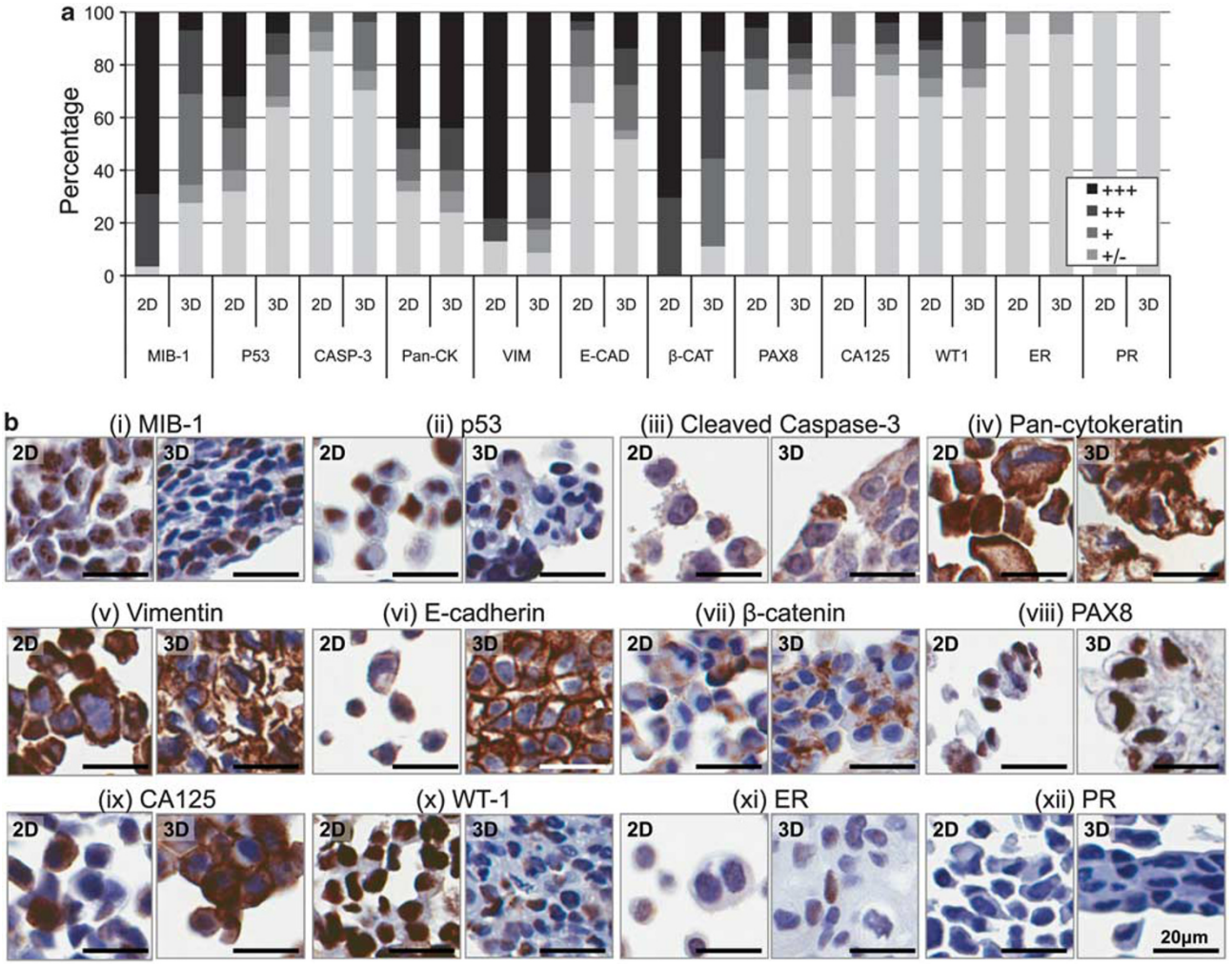

Figure 5 Analysis of histological features and expression of ovarian cancer biomarkers in two- (2D) and three-dimensional (3D). Tissue microarrays (TMAs) of the epithelial ovarian cancers (EOCs) cultured in 2D and 3D conditions were generated, and immunohistochemistry for the indicated markers was performed. (**a**) Quantification of positively stained cells for each biomarker. Data are represented as the frequency of each score for 2D- or 3D-cultured cells. $+++$, $>75\%$ of cells stained positive; $++$, 25–75% of cells stained positive; $+<25\%$ of cells stained positive; $+/-$, weak staining in $<10\%$ of cells; $-$, no positively stained cells. CASP-3, cleaved caspase-3; PAN-CK, pan-cytokeratin; VIM, vimentin; E-CAD, E-cadherin; β-CAT, β-catenin; WT1, Wilms Tumor protein 1; ER, estrogen receptor; PR progesterone receptor. (**b**) Representative stained cultures from the TMA. (i) SKOV3 cells stained for MIB1. 2D cultured cells are $>95\%$ positive, in 3D-cultured cells positively staining cells are predominantly located at the edge of the multicellular aggregate (MCA). (ii) P53 expression in 2D- and 3D-cultured EFO27 cells, expression is lower in 3D. Detection of P53 did not correlate with the mutation status of each cell line (Table 1). (iii) Cleaved caspase 3 expression in A2780.CP cells is higher in 3D cultures than in 2D. (iv) Pan-cytokeratin (clone AE1/AE3) expression in OAW42 low-grade serous EOC cells is high in both 2D and in 3D culture systems. (v) Vimentin expression in TOV21G cells is slightly increased when cells are maintained in a 3D microenvironment. (vi) E-cadherin expression is upregulated in 3D-cultured OV2008 cells compared with the same cells cultured as monolayers. E-cadherin expression is localized to the cell membrane. (vii) β-catenin expression in IGROV1 cells is localized to the cell membrane in 2D cultured cells and in 3D tends to be restricted to the outer edge of MCAs. (viii) PAX8 expression in OAW42 cells is higher following a transition to a 3D microenvironment. (ix) CA125 expression is upregulated in 3D-cultured CaOV3 cells relative to the same cells cultured in 2D. (x) WT1 expression in COV434 cells is downregulated in 3D culture. (xi) OV2008 cells express nuclear estrogen receptor (ER) alpha in $<25\%$ of cells in both 2D and 3D. (xii) None of the EOC cell lines tested express progesterone receptor (PR). Brown color indicates positive antigen staining, cells are counterstained with hematoxylin (blue). Brightfield microscopy.

Differential Rates of Proliferation in 2D and 3D-Cultured EOC Cells

We analyzed proliferation rates in nine different cell lines, three lines from each of the three morphological groups, cultured in both 2D and 3D. Six lines were significantly more proliferative in 2D compared with 3D ($P<1\times10^{-4}$, two-way ANOVA, Figures 6a–c); the lines 1847 and A2780 showed no significant differences in proliferation in 2D and 3D microenvironments, and IGROV1 was the only cell line that was more proliferative in 3D than in 2D ($P<1\times10^{-4}$, two-way ANOVA, Figure 6b). The lower proliferation rates in 3D cultures are consistent with the lower proliferative indices we observed by MIB1 staining by IHC staining of the TMAs. The most prominent differences in growth rates were in LDAs and

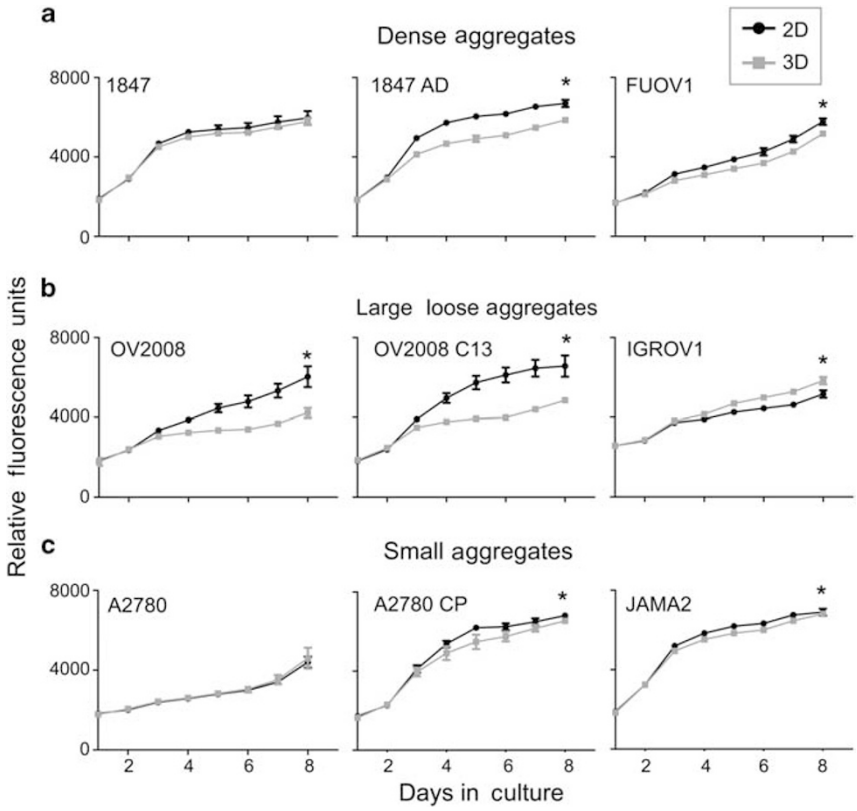

Figure 6 Differential proliferation rates of epithelial ovarian cancer (EOC) cell lines maintained in two- (2D) and three-dimensional (3D) culture systems. Cell lines from each group of multicellular aggregates (**a**) large dense, (**b**) large loose and (**c**) small aggregates were cultured in 2D and 3D and proliferative rates measured. By a two-way ANOVA test, six of the nine cell lines tested were significantly less proliferative in 3D conditions while the IGROV1 line was significantly more proliferative in 3D conditions (*$P<0.0001$).

LLAs, suggesting that there is a relationship between MCA structure and size and cell proliferation.

3D-Cultured EOC Cell Lines are More Chemoresistant

We evaluated chemosensitivity in 3D compared with 2D in 11 cell lines representing the three MCA morphological groups, by culturing these lines in two standard chemotherapeutic agents for ovarian cancer, cisplatin, and paclitaxel. When treated with cisplatin seven out of 11 cell lines tested showed a significant increase in survival of up to 30% in 3D models compared with 2D cultures ($P>0.05$, two-tailed paired Student's *t*-test, Figure 7a). Seven of the 11 cell lines tested also displayed increased resistance to paclitaxel in 3D cultures compared with 2D ($P>0.05$, two-tailed paired Student's *t*-test. Figure 6b). The LDAs and LLAs tended to show the greatest changes in survival in the presence of cisplatin or paclitaxel compared with the lines that formed SAs.

DISCUSSION

In the current study, we established and characterized 31 different EOC cell lines as 3D *in vitro* models. We compared the biological and molecular features of cells grown in 3D with 2D cultured counterparts, with xenografts and with primary ovarian tumors, and tested their efficacy as models for evaluating chemoresponse using the standard first-line chemotherapy for EOC. Although the chemoresponse of the NCI-60 panel of cell lines in 3D has been studied,[17] to our knowledge, this represents the largest systematic phenotypic characterization of 3D-cultured ovarian cancer cell lines. The methodologies we present combine high-throughput 3D drug screening with analysis of biomarker expression and the ability to rapidly screen multiple cell lines grown as 3D spheroids, concurrently evaluating pathway activation and response to novel therapeutic agents, and represent an ideal system for the discovery and development of novel targeted therapies.

We used polyHEMA coating of tissue culture plastics to establish 3D spheroid cultures of cell lines. Different approaches to *in vitro* 3D modeling have been used previously, including gel- or scaffold-based cultures.[50–55] These approaches have mainly been used for studies of cell invasion[51,52] and metastasis to the omentum[53,54] and have typically low throughput. The characteristics of the 3D EOC aggregates we describe here resemble those previously reported for some of the cell lines used in this study (TOV112D, TOV21G, OVCAR5, SKOV3, HEY, ES-2[50,52,54]), although some of our cell lines also behaved differently. For example, the OVCA433 and OVCA429 lines did not form

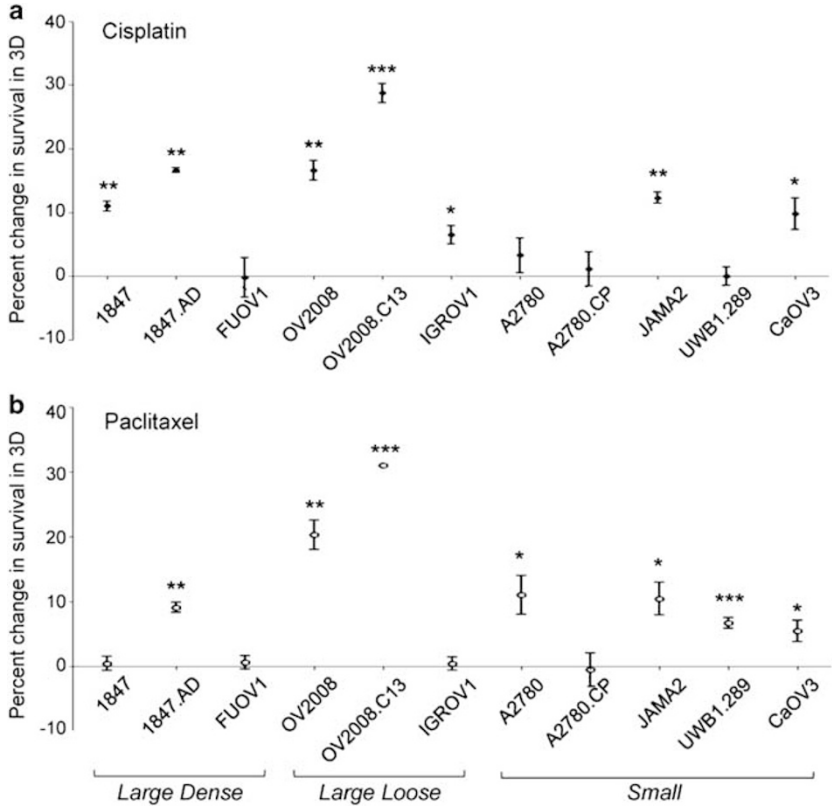

Figure 7 Differential response of two- (2D) and three-dimensional (3D)-cultured epithelial ovarian cancer (EOC) cells to chemotherapy. Eleven EOCs cultured in 2D and 3D conditions were challenged with sublethal doses of (**a**) cisplatin (0.1 mg/ml) and (**b**) paclitaxel (100 nM) and the survival rates measured. 3D culturing was associated with increased resistance to both agents. Results are representative of at least three independent experiments. $^{*}P > 0.05$; $^{**}P > 0.01$, $^{***}P > 0.001$, two-tailed paired Student's *t*-test, with assumed equal variance. Mean ± standard error of the mean is shown, graphs are representative of three independent experiments.

spheroids in the present study but have been shown to form 3D structures *in vitro* in other studies.[54,55] This may reflect the different 3D culture techniques used in different laboratories or clonal variation present across various strains of cell lines.

All but two cell lines grew as 3D aggregates. Many lines displayed a striking level of histological differentiation in 3D that was not seen for the same lines grown in 2D, suggesting that the signaling involved in establishing the differentiated structures can be restored even after prolonged culture in 2D. MCAs could be sub-categorized based on their gross morphological and histological features, into LDAs, LLAs or SAs. These groupings were reproducible when EOC cell lines were analyzed at different passages. Western blotting and IHC identified several molecular changes resulting from culturing cells in 3D compared with 2D. Many of these changes indicated that 3D cultures better reflected the molecular characteristics of primary tumors; for example, reduced MIB1 expression and increased E-cadherin, PAX8, and CA125 expression. Overall, cytokeratin and E-cadherin, which are commonly expressed in advanced ovarian tumors,[56–58] were upregulated in 3D, whereas vimentin tended to be downregulated, suggesting that many EOC cell lines underwent mesenchymal-to-epithelial transition in 3D which reflects the acquisition of a differentiated phenotype that more closely reflects the protein expression in primary tumors. In this regard EOCs are in contrast to most other solid tumors, which undergo an epithelial-to-mesenchymal transition during neoplastic progression.[57,59] We observed heterogeneity in marker expression within the different 3D groups; nonetheless there were some trends between MCA morphology and protein expression. Cell lines that formed LDAs tended to be epithelial-type EOC cells, whereas large loose and small MCAs were formed by both mesenchymal-type cell lines and epithelial-type EOC lines.

The main advantage of these models is the ability to restore the histological differentiation of primary ovarian carcinomas. EOCs are a heterogeneous group of tumors in which the four main subtypes (serous, endometrioid, mucinous, and clear cell) have such distinct histological, molecular, clinical, and etiological characteristics that they can be considered to be different diseases.[49] However, most research that utilizes *in vitro* models of EOC largely ignores the histological characteristics or origins of EOC cell lines,

often because these data are not available. In some cases, we observed histological differentiation of cell lines derived from tumors previously described as of unknown histology. For example, SKOV3 is the most widely used *in vitro* model for studying ovarian cancer; but our data show that the characteristics of the SKOV3ip line in 3D bears striking histological resemblance to a clear cell ovarian cancer, which is the least common histological subtype of invasive disease. Conversely, some cell lines of known histology resembled poorly differentiated carcinomas in 3D, suggesting that these cell lines may have become dedifferentiated following extended passaging *in vitro*. The ability to determine underlying histotype for some of the most commonly used EOC cell lines and therefore generate subtype-specific models for EOC represents a significant advance, which could have implications for understanding the development of the different subtypes of disease.

One of the major challenges in the treatment of many tumor types is acquired chemoresistance to existing therapies. There have been considerable advances in targeted therapies for some tumor types, notably trastuzumab targeting *HER2* amplification in breast cancers.[60] However, for EOC there is a pressing clinical need to identify and develop novel therapeutic approaches to treat or circumvent chemorefractory recurrent disease. In this study, we found overwhelming evidence that EOC cells cultured in 3D show increased resistance to both a DNA-damaging agent (cisplatin) and a microtubule-stabilizing agent (paclitaxel). This is the first large-scale analysis of chemoresponse in EOC cell lines comparing 2D and 3D microenvironments, and the results are consistent with smaller studies.[61–65] Previous studies in other tumor types have also shown resistance to chemotherapy and targeted therapies is enhanced in 3D culture models.[61,63] It is also worth noting that the commonly used chemoresistant/chemosensitive ovarian cancer cell line pairs are generated by culturing cells as monolayers in the presence of drug; the 3D-culturing method used here represents a more physiologically relevant model for the generation of novel drug-resistant lines. The mechanisms underlying increased resistance in 3D models are not yet well understood, but it is possible that changes in gene expression, the presence of hypoxic zones, and/or reduced penetration of drug into the central areas of MCAs are contributory factors. We did not observe statistically significant changes in proliferation occurring within the 48-h timecourse of the drug assays, suggesting differential rates of proliferation are not driving the differential chemoresponse of 3D cultures. The overall trend for increased resistance to therapies in 3D suggests that this may represent a more reliable approach to testing the efficacy of novel therapeutic targets, rather than 2D approaches that are currently used in high-throughput drug discovery pipelines.

In conclusion, this study shows that 3D models of ovarian cancers more accurately reflect the characteristics of primary human EOCs *in vivo* and in xenograft than 2D monolayer cultures of the same cell lines, and so these models are likely to represent better *in vitro* approaches for studying the underlying biology of the disease. Perhaps more significantly, we present a high-throughput approach to histological classification of ovarian cancer cell lines grown in 3D. Given the relative failure of existing 2D approaches to drug discovery for EOC and the observed difference in chemosensitivity between 2D and 3D, it may be that 3D models represent a more efficacious first-line approach to identify novel drug targets for EOC in the future. Adoption of these techniques during preclinical drug development may help to reduce numbers of animals used in the testing of new anti-cancer therapeutics. Finally, although we have focused on ovarian cancer in this study, the techniques and methodological approaches could be readily applied to the study of any solid tumor type.

Supplementary Information accompanies the paper on the Laboratory Investigation website (http://www.laboratoryinvestigation.org)

ACKNOWLEDGEMENTS

We would like to thank Alexa Trana for tissue microarray construction and Lillian Young for immunohistochemistry services.

Grant Support: KL is funded by National Institute of Health grant number 5 U19 CA148112-02 and an Ann Schreiber Program of Excellence award from the Ovarian Cancer Research Fund. This work was performed within the Norris Comprehensive Cancer Center (NCI CCSG grant P30CA014089). This work was in part supported by the Genetic Associations and Mechanisms in Oncology (GAME-ON) consortium: a NCI Cancer Post-GWAS Initiative (U19-CA148112).

DISCLOSURE/CONFLICT OF INTEREST

The authors declare no conflict of interest.

1. Ashworth A, Balkwill F, Bast RC, *et al.* Opportunities and challenges in ovarian cancer research, a perspective from the 11th Ovarian Cancer Action/HHMT Forum, Lake Como, March 2007. Gynecol Oncol 2008;108:652–657.
2. Ma XH, Piao S, Wang D, *et al.* Measurements of tumor cell autophagy predict invasiveness, resistance to chemotherapy, and survival in melanoma. Clin Cancer Res 2011;17:3478–3489.
3. Smalley KS, Haass NK, Brafford PA, *et al.* Multiple signaling pathways must be targeted to overcome drug resistance in cell lines derived from melanoma metastases. Mol Cancer Ther 2006;5:1136–1144.
4. dit Faute MA, Laurent L, Ploton D, *et al.* Distinctive alterations of invasiveness, drug resistance and cell-cell organization in 3D-cultures of MCF-7, a human breast cancer cell line, and its multidrug resistant variant. Clin Exp Metastasis 2002;19:161–168.
5. Weigelt B, Lo AT, Park CC, *et al.* HER2 signaling pathway activation and response of breast cancer cells to HER2-targeting agents is dependent strongly on the 3D microenvironment. Breast Cancer Res Treat 2010;122:35–43.
6. Barcellos-Hoff MH, Aggeler J, Ram TG, *et al.* Functional differentiation and alveolar morphogenesis of primary mammary cultures on reconstituted basement membrane. Development 1989;105:223–235.
7. T, Tokuda Y, Nakamura Y, Suzuki A, *et al.* A new high-yield continuous cell-culture system for lymphokine-activated killer cells. Cancer Immunol Immunother 1989;30:1–4.
8. Khaoustov VI, Darlington GJ, Soriano HE, *et al.* Induction of three-dimensional assembly of human liver cells by simulated microgravity. In Vitro Cell Dev Biol Anim 1999;35:501–509.

9. Lawrenson K, Benjamin E, Turmaine M, *et al.* In vitro three-dimensional modelling of human ovarian surface epithelial cells. Cell Prolif 2009;42:385–393.
10. Hutmacher DW. Scaffold design and fabrication technologies for engineering tissues–state of the art and future perspectives. J Biomater Sci Polym Ed 2001;12:107–124.
11. Ghosh S, Spagnoli GC, Martin I, *et al.* Three-dimensional culture of melanoma cells profoundly affects gene expression profile: a high density oligonucleotide array study. J Cell Physiol 2005;204: 522–531.
12. Gómez-Lechón MJ, Jover R, Donato T, *et al.* Long-term expression of differentiated functions in hepatocytes cultured in three-dimensional collagen matrix. J Cell Physiol 1998;177:553–562.
13. Delcommenne M, Streuli CH. Control of integrin expression by extracellular matrix. J Biol Chem 1995;270:26794–26801.
14. Kenny PA, Lee GY, Myers CA, *et al.* The morphologies of breast cancer cell lines in three-dimensional assays correlate with their profiles of gene expression. Mol Oncol 2007;1:84–96.
15. Rohwer N, Cramer T. Hypoxia-mediated drug resistance: novel insights on the functional interaction of HIFs and cell death pathways. Drug Resist Update 2011;14:191–201.
16. Vinci M, Gowan S, Boxall F, *et al.* Advances in establishment and analysis of three-dimensional tumor spheroid-based functional assays for target validation and drug evaluation. BMC Biol 2012;10:29.
17. Friedrich J, Seidel C, Ebner R, *et al.* Spheroid-based drug screen: considerations and practical approach. Nat Protoc 2009;4:309–324.
18. Audeh MW, Carmichael J, Penson RT, *et al.* Oral poly(ADP-ribose) polymerase inhibitor olaparib in patients with BRCA1 or BRCA2 mutations and recurrent ovarian cancer: a proof-of-concept trial. Lancet 2010;376:245–251.
19. Wright JD, Secord AA, Numnum TM, *et al.* A multi-institutional evaluation of factors predictive of toxicity and efficacy of bevacizumab for recurrent ovarian cancer. Int J Gynecol Cancer 2008;18:400–406.
20. Agarwal R, Kaye SB. Ovarian cancer: strategies for overcoming resistance to chemotherapy. Nat Rev Cancer 2003;3:502–516.
21. Eva A, Robbins KC, Andersen PR, *et al.* Cellular genes analogous to retroviral onc genes are transcribed in human tumour cells. Nature 1982;295:116–119.
22. Godwin AK, Meister A, O'Dwyer PJ, *et al.* High resistance to cisplatin in human ovarian cancer cell lines is associated with marked increase of glutathione synthesis. Proc Natl Acad Sci USA 1992;89:3070–3074.
23. Louie KG, Behrens BC, Kinsella TJ, *et al.* Radiation survival parameters of antineoplastic drug-sensitive and -resistant human ovarian cancer cell lines and their modification by buthionine sulfoximine. Cancer Res 1985;45:2110–2115.
24. Buick RN, Pullano R, Trent JM, *et al.* Comparative properties of five human ovarian adenocarcinoma cell lines. Cancer Res 1985;45: 3668–3676.
25. van den Berg-Bakker CA, Hagemeijer A, Franken-Postma EM, *et al.* Establishment and characterization of 7 ovarian carcinoma cell lines and one granulosa tumor cell line: growth features and cytogenetics. Int J Cancer 1993;53:613–620.
26. Simon WE, Albrecht M, Hänsel M, *et al.* Cell lines derived from human ovarian carcinomas: growth stimulation by gonadotropic and steroid hormones. J Natl Cancer Inst 1983;70:839–845.
27. Lau DH, Lewis AD, Ehsan MN, *et al.* Multifactorial mechanisms associated with broad cross-resistance of ovarian carcinoma cells selected by cyanomorpholino doxorubicin. Cancer Res 1991;51: 5181–5187.
28. Mills GB, May C, Hill M, *et al.* Ascitic fluid from human ovarian cancer patients contains growth factors necessary for intraperitoneal growth of human ovarian adenocarcinoma cells. J Clin Invest 1990;86: 851–855.
29. Bénard J, Da Silva J, De Blois MC, *et al.* Characterization of a human ovarian adenocarcinoma line, IGROV1, in tissue culture and in nude mice. Cancer Res 1985;45:4970–4979.
30. Ward BG, Wallace K, Shepherd JH, *et al.* Intraperitoneal xenografts of human epithelial ovarian cancer in nude mice. Cancer Res 1987;47:2662–2667.
31. Mistry P, Kelland LR, Abel G, *et al.* The relationships between glutathione, glutathione-S-transferase and cytotoxicity of platinum drugs and melphalan in eight human ovarian carcinoma cell lines. Br J Cancer 1991;64:215–220.
32. Wilson AP. Characterization of a cell line derived from the ascites of a patient with papillary serous cystadenocarcinoma of the ovary. J Natl Cancer Inst 1984;72:513–521.
33. Alama A, Barbieri F, Favre A, *et al.* Establishment and characterization of three new cell lines derived from the ascites of human ovarian carcinomas. Gynecol Oncol 1996;62:82–88.
34. DiSaia PJ, Sinkovics JG, Rutledge FN, *et al.* Cell-mediated immunity to human malignant cells. A brief review and further studies with two gynecologic tumors. Am J Obstet Gynecol 1972;114:979–989.
35. Andrews PA, Albright KD. Mitochondrial defects in cis-diamminedichloroplatinum(II)-resistant human ovarian carcinoma cells. Cancer Res 1992;52:1895–1901.
36. Bast Jr RC, Feeney M, Lazarus H, *et al.* Reactivity of a monoclonal antibody with human ovarian carcinoma. J Clin Invest 1981;68: 1331–1337.
37. Hamilton TC, Young RC, McKoy WM, *et al.* Characterization of a human ovarian carcinoma cell line (NIH:OVAR-3) with androgen and estrogen receptors. Cancer Res 1983;43:5379–5389.
38. Hamilton TC, Lai GM, Rothenberg ML, *et al.* Mechanisms of resistance to cisplatin and alkylating agents. Cancer Treat Res 1989;48:151–169.
39. Möbus VJ, Moll R, Gerharz CD, *et al.* Establishment of new ovarian and colon carcinoma cell lines: differentiation is only possible by cytokeratin analysis. Br J Cancer 1994;69:422–428.
40. Hills CA, Kelland LR, Abel G, *et al.* Biological properties of ten human ovarian carcinoma cell lines: calibration in vitro against four platinum complexes. Br J Cancer 1989;59:527–534.
41. Yu D, Wolf JK, Scanlon M, *et al.* Enhances c-erbB-2/neu expression in human ovarian cancer cells correlates with more severe malignancy that can be suppressed by E1A. Cancer Res 1993;53: 891–898.
42. Provencher DM, Lounis H, Champoux L, *et al.* Characterization of four novel epithelial ovarian cancer cell lines. In Vitro Cell Dev Biol Anim 2000;36:357–361.
43. DelloRusso C, Welcsh PL, Wang W, *et al.* Functional characterization of a novel BRCA1-null ovarian cancer cell line in response to ionizing radiation. Mol Cancer Res 2007;5:35–45.
44. Kühn W, Kaufmann M, Feichter GE, *et al.* DNA flow cytometry, clinical and morphological parameters as prognostic factors for advanced malignant and borderline ovarian tumors. Gynecol Oncol 1989;33:360–367.
45. Shaw TJ, Senterman MK, Dawson K, *et al.* Characterization of intraperitoneal, orthotopic, and metastatic xenograft models of human ovarian cancer. Mol Ther 2004;10:1032–1042.
46. Korch C, Spillman MA, Jackson TA, *et al.* DNA profiling analysis of endometrial and ovarian cell lines reveals misidentification, redundancy and contamination. Gynecol Oncol 2012;127: 241–248.
47. Faleiro-Rodrigues C, Macedo-Pinto I, Pereira D, *et al.* Prognostic value of E-cadherin immunoexpression in patients with primary ovarian carcinomas. Ann Oncol 2004;15:1535–1542.
48. Davies BR, Worsley SD, Ponder BA. Expression of E-cadherin, alpha-catenin and beta-catenin in normal ovarian surface epithelium and epithelial ovarian cancers. Histopathology 1998;32:69–80.
49. Köbel M, Kalloger SE, Boyd N, *et al.* Ovarian carcinoma subtypes are different diseases: implications for biomarker studies. PLoS Med 2008;5:e232.
50. Zietarska M, Maugard CM, Filali-Mouhim A, *et al.* Molecular description of a 3D in vitro model for the study of epithelial ovarian cancer (EOC). Mol Carcinog 2007;46:872–885.
51. Barbolina MV, Adley BP, Kelly DL, *et al.* Downregulation of connective tissue growth factor by three-dimensional matrix enhances ovarian carcinoma cell invasion. Int J Cancer 2009;125:816–825.
52. Sodek KL, Ringuette MJ, Brown TJ. Compact spheroid formation by ovarian cancer cells is associated with contractile behavior and an invasive phenotype. Int J Cancer 2009;124:2060–2070.
53. Kenny HA, Krausz T, Yamada SD, *et al.* Use of a novel 3D culture model to elucidate the role of mesothelial cells, fibroblasts and extra-cellular matrices on adhesion and invasion of ovarian cancer cells to the omentum. Int J Cancer 2007;121:1463–1472.
54. Iwanicki MP, Davidowitz RA, Ng MR, *et al.* Ovarian cancer spheroids use myosin-generated force to clear the mesothelium. Cancer Discov 2011;1:144–157.

55. Shepherd TG, Mujoomdar ML, Nachtigal MW. Constitutive activation of BMP signalling abrogates experimental metastasis of OVCA429 cells via reduced cell adhesion. J Ovarian Res 2010;3:5.
56. Kwon Y, Cukierman E, Godwin AK. Differential expressions of adhesive molecules and proteases define mechanisms of ovarian tumor cell matrix penetration/invasion. PLoS One 2011;6:e18872.
57. Sundfeldt K. Cell-cell adhesion in the normal ovary and ovarian tumors of epithelial origin; an exception to the rule. Mol Cell Endocrinol 2003;202:89–96.
58. Sundfeldt K, Piontkewitz Y, Ivarsson K, *et al.* E-cadherin expression in human epithelial ovarian cancer and normal ovary. Int J Cancer 1997;74:275–280.
59. Dabbs DJ, Geisinger KR. Common epithelial ovarian tumors. Immunohistochemical intermediate filament profiles. Cancer 1988;62:368–374.
60. Goldenberg MM. Trastuzumab, a recombinant DNA-derived humanized monoclonal antibody, a novel agent for the treatment of metastatic breast cancer. Clin Ther 1999;21:309–318.
61. Yang Z, Zhao X. A 3D model of ovarian cancer cell lines on peptide nanofiber scaffold to explore the cell-scaffold interaction and chemotherapeutic resistance of anticancer drugs. Int J Nanomedicine 2011;6:303–310.
62. Rizvi I, Celli JP, Evans CL, *et al.* Synergistic enhancement of carboplatin efficacy with photodynamic therapy in a three-dimensional model for micrometastatic ovarian cancer. Cancer Res 2010;70:9319–9328.
63. Rahmanzadeh R, Rai P, Celli JP, *et al.* Ki-67 as a molecular target for therapy in an in vitro three-dimensional model for ovarian cancer. Cancer Res 2010;70:9234–9242.
64. Evans CL, Abu-Yousif AO, Park YJ, *et al.* Killing hypoxic cell populations in a 3D tumor model with EtNBS-PDT. PLoS One 2011;6:e23434.
65. Loessner D, Stok KS, Lutolf MP, *et al.* Bioengineered 3D platform to explore cell-ECM interactions and drug resistance of epithelial ovarian cancer cells. Biomaterials 2010;31:8494–8506.